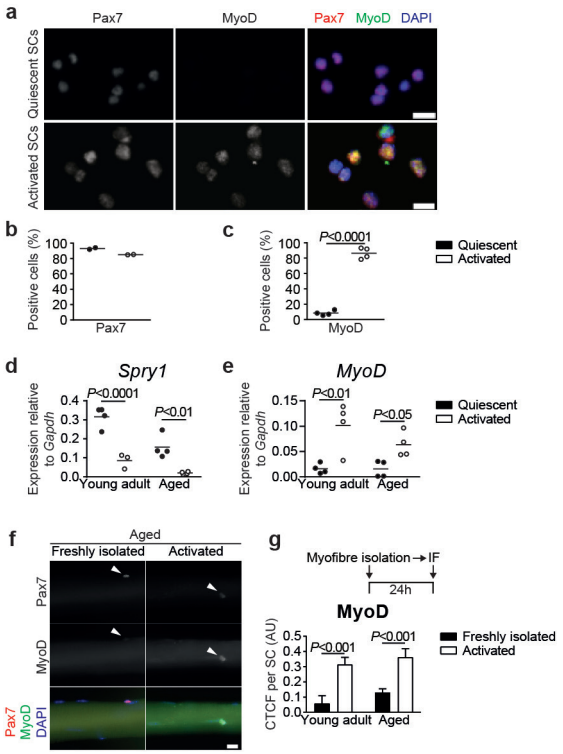

Extended Data Figure 1 | SC activation. a, Immunofluorescence staining for Pax7 and MyoD of freshly isolated SCs from injured (activated SCs) and uninjured muscles (quiescent SCs) from young adult mice. Nuclei were counterstained with DAPI (blue). **b**, **c**, Quantification of Pax7$^+$ cells (**b**) and MyoD$^+$ cells (**c**) in **a**. **d**, **e**, qPCR analysis of *Spry1* (**d**) and *Myod1* (**e**) expression in freshly isolated quiescent and *in vivo* activated SCs of young adult and aged mice. **f**, Immunofluorescence staining for Pax7 and MyoD on freshly isolated and 24-h cultured myofibre-associated SCs from aged mice. Nuclei were counterstained with DAPI (blue). **g**, Corrected total cell fluorescence (CTCF) for MyoD per SC as in **f**. Scale bars, 10 μm (**a**) and 20 μm (**f**). *P* values were calculated by two-sided Student's *t*-test (**b**, **c**) or two-way ANOVA (**d**, **e**, **g**). $n = 2$ mice in **b**; $n = 4$ mice in **c**; $n = 3$ mice (young activated), $n = 4$ mice (all others) in **d**; $n = 4$ mice in **e**; $n = 33/24$ nuclei (young), $n = 35/20$ nuclei (aged) from 3 mice in **g**.

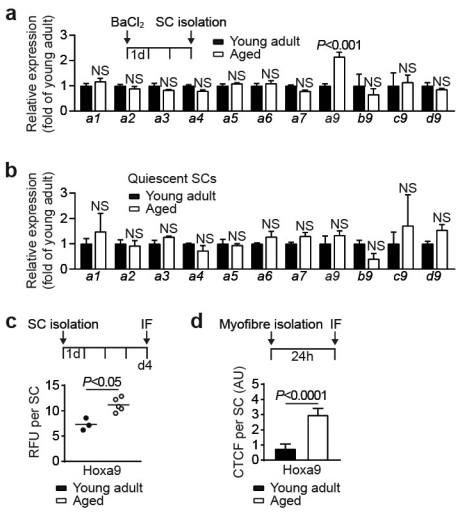

Extended Data Figure 2 | Expression of Hox genes in SCs. a, **b**, Nanostring analysis of mRNA expression of *Hoxa* genes and *Hoxa9* paralogues (*b9-c9-d9*) in *in vivo* activated (**a**) and quiescent (**b**) freshly isolated SCs from young adult and aged mice. **c**, Relative fluorescence units (RFU) for Hoxa9 per SC in 4-day cultured SCs from young adult and aged mice. **d**, Corrected total cell fluorescence (CTFC) for Hoxa9 per activated SC on 24-h cultured myofibres as in Fig. 1d. *P* values were calculated by two-way ANOVA (**a**, **b**) or two-sided Mann–Whitney *U*-test (**c**, **d**). $n = 3$ mice in **a**, **b**; $n = 3$ mice (young), $n = 5$ mice (aged) in **c**; $n = 34$ nuclei (young), $n = 32$ nuclei (aged) from 4 mice in **d**.

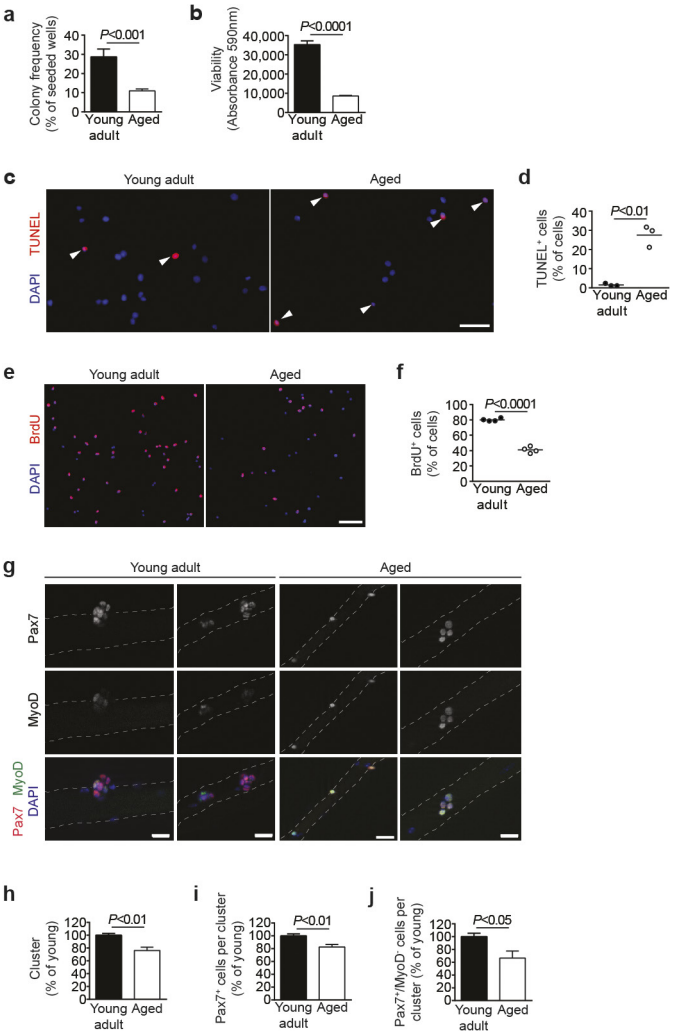

Extended Data Figure 3 | Functional decline in aged SCs. a, SCs from young adult and aged mice were sorted as single cells. After 5 days, the frequency of myogenic colonies was assessed. **b**, Equal numbers of FACS-isolated SCs from young adult and aged mice were cultured for 4 days and Alamar Blue assay was performed. **c**, TUNEL staining of SCs isolated from young adult or aged mice after 4 days of culture. Nuclei were counterstained with DAPI (blue). **d**, Quantification of apoptosis based on TUNEL staining in **c**. **e**, BrdU staining of SCs isolated from young adult or aged mice after 4 days of culture. Nuclei were counterstained with DAPI (blue). **f**, Quantification of proliferation based on BrdU staining in **e**. **g**, Immunofluorescence staining for Pax7 and MyoD on myofibres isolated from young adult and aged mice after 72 h in culture. Nuclei were counterstained with DAPI (blue). **h**–**j**, Quantification of the number of SC-derived clusters with at least 3 adjacent cells (**h**), average number of all Pax7$^+$ cells (**i**), or proportion of Pax7$^+$/MyoD$^-$ cells (**j**) within clusters as in **g**. Scale bars, 20 μm (**c**, **g**) and 50 μm (**e**). *P* values were calculated by two-sided Student's *t*-test. $n = 8$ mice (young), $n = 10$ mice (aged) in **a**; $n = 7$ mice (young), $n = 5$ mice (aged) in **b**; $n = 3$ mice in **d**; $n = 4$ mice in **f**; $n = 4$ mice (aged) in **j**, $n = 5$ mice (all others) in **h**–**j**.

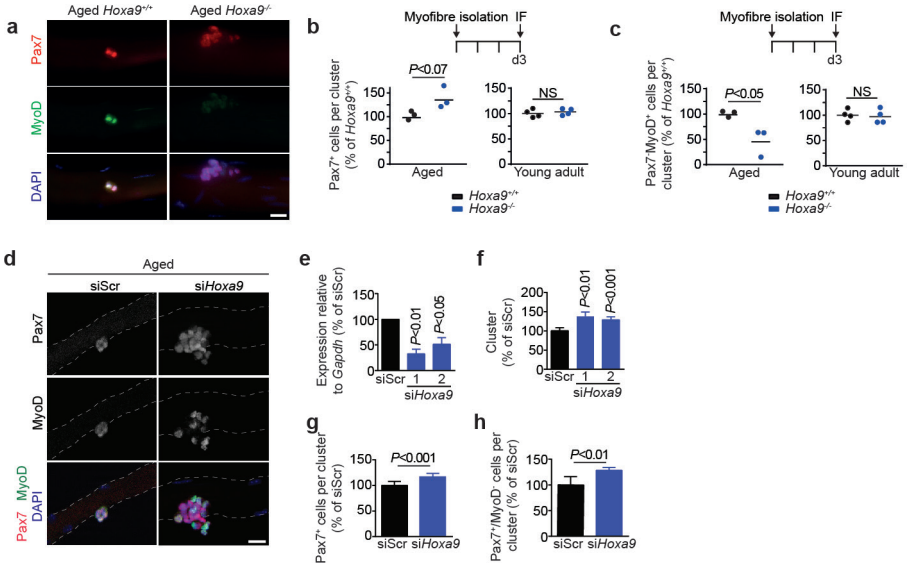

Extended Data Figure 4 | Deletion or knockdown of Hoxa9 improves SC function in myofibre cultures. a, Immunofluorescence staining for Pax7 and MyoD on 72 h cultured myofibre-associated SCs from aged *Hoxa9*$^{+/+}$ and *Hoxa9*$^{-/-}$ mice. **b**, **c**, Average number of all Pax7^{+} cells (**b**) or Pax7^{-}/MyoD^{+} cells (**c**) within clusters from aged or young adult *Hoxa9*$^{+/+}$ and *Hoxa9*$^{-/-}$ mice as shown in **a**. **d**, Immunofluorescence staining for Pax7 and MyoD on 72-h cultured myofibres isolated from aged mice transfected with *Hoxa9* or scrambled (Scr) siRNAs. Nuclei were counterstained with DAPI (blue). **e**, qPCR analysis of *Hoxa9* expression in SCs transfected with *Hoxa9* siRNA or scrambled control. Two *Hoxa9* siRNAs with different target sequences (Supplementary Table 1) were used. **f**–**h**, Analysis of 72-h cultured myofibre-associated SCs from **d**. Quantification of the number of SC-derived clusters with at least 3 adjacent cells (**f**), average number of all Pax7^{+} cells (**g**), or proportion of Pax7^{+}/MyoD^{-} cells (**h**) within clusters. Scale bars, 20 μm (**a**, **d**). Dashed lines outline myofibres. *P* values were calculated by two-sided Student's *t*-test. $n = 3$ mice (aged), $n = 4$ mice (young) in **b**, **c**; $n = 3$ mice in **e**; $n = 5$ mice in **f**–**h**.

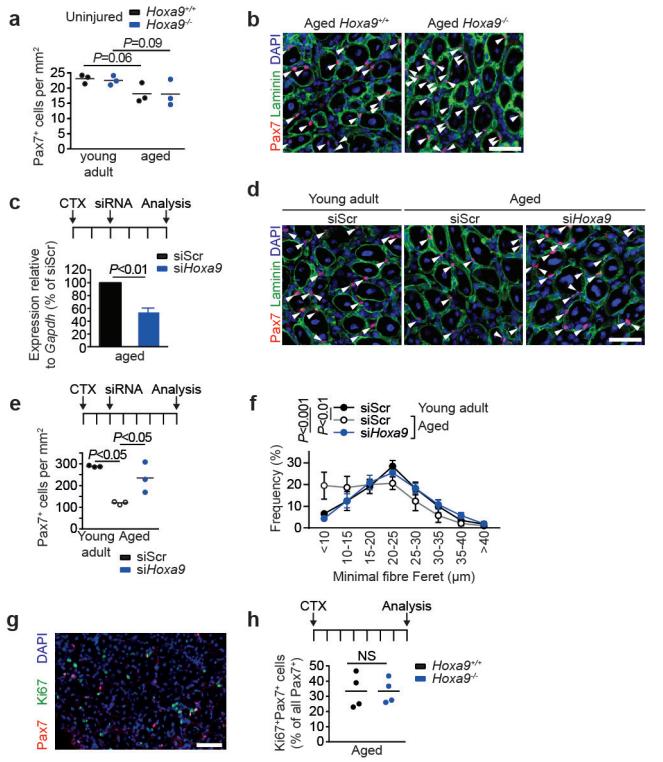

Extended Data Figure 5 | Inhibition of *Hoxa9* improves muscle regeneration in aged mice. **a**, Quantification of Pax7$^+$ cells per area in uninjured tibialis anterior muscles from young adult and aged *Hoxa9*$^{+/+}$ and *Hoxa9*$^{-/-}$ mice. **b**, Representative immunofluorescence staining for Pax7 and laminin on tibialis anterior muscles from aged *Hoxa9*$^{+/+}$ and *Hoxa9*$^{-/-}$ mice that were collected 7 days after cardiotoxin (CTX) injury. **c**, qPCR analysis of *Hoxa9* expression in SCs isolated from tibialis anterior muscles injected with a self-delivering *Hoxa9* or scrambled siRNA and collected 5 days after muscle injury. **d**, Representative immunofluorescence staining for Pax7 and laminin of injured tibialis anterior muscles from young adult and aged mice that were injected with a self-delivery siRNA and collected 7 days after muscle injury. Nuclei were counterstained with DAPI (blue). Arrowheads denote Pax7$^+$ cells. **e**, Quantification of Pax7$^+$ cells from **d** per area. **f**, Frequency distribution minimal Feret's diameter of muscle fibres from **d**. **g**, Exemplary immunofluorescence staining for Pax7 and Ki67 on tibialis anterior muscles from aged *Hoxa9*$^{+/+}$ and *Hoxa9*$^{-/-}$ mice collected 7 days after muscle injury. Nuclei were counterstained with DAPI (blue). **h**, Quantification of proliferating SCs (Ki67$^+$/Pax7$^+$) as depicted in **g**. Scale bars, 50 µm. *P* values were calculated by two-sided Student's *t*-test (**c**, **h**) or two-way ANOVA (**a**, **e**, **f**). $n = 3$ mice in **a**; $n = 3$ mice in **c**; $n = 3$ mice in **e**, **f**; $n = 4$ mice in **h**.

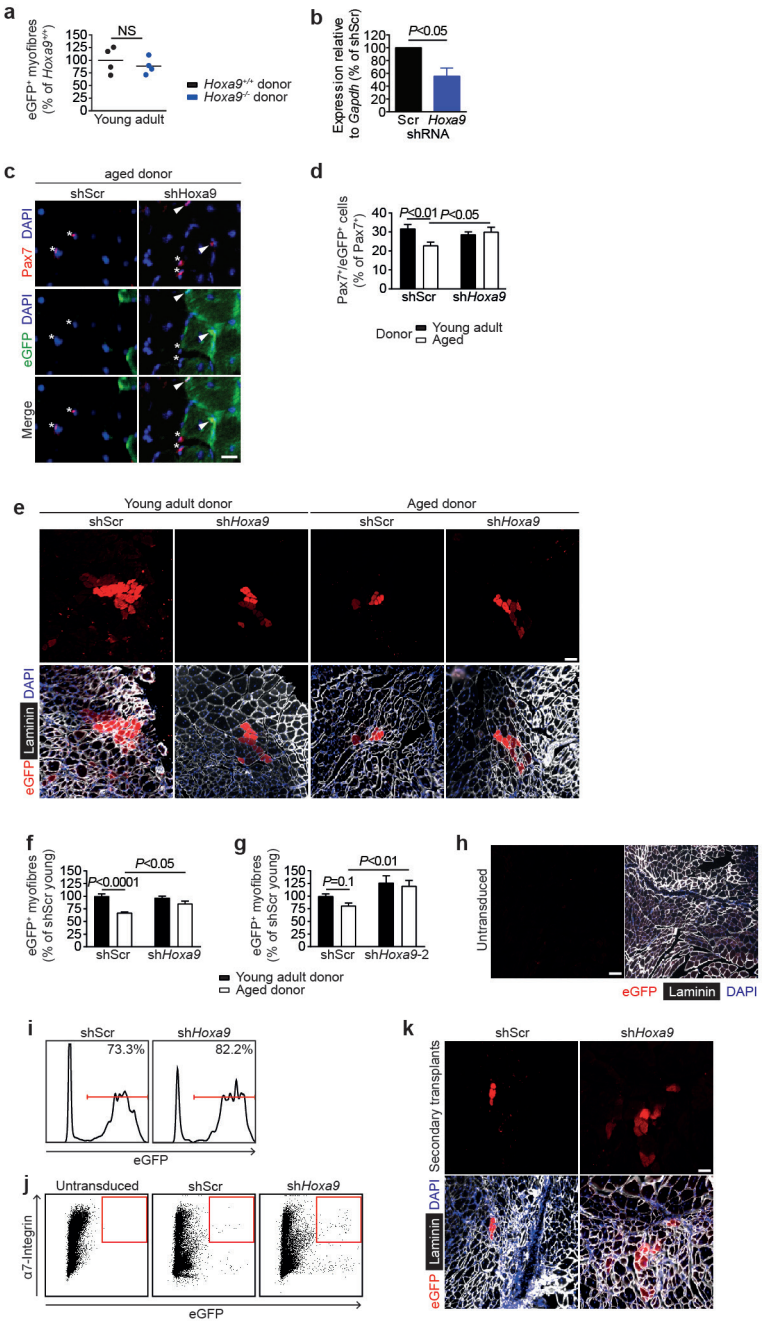

Extended Data Figure 6 | Inhibition of *Hoxa9* improves regenerative capacity of aged SCs. a, Quantification of donor-derived (eGFP$^+$) myofibres from transplantation of SCs from young adult *Hoxa9*$^{+/+}$ and *Hoxa9*$^{-/-}$ mice. **b**, qPCR analysis of *Hoxa9* expression in SCs transduced with scrambled control or *Hoxa9* shRNA encoding lentivirus. **c**–**g**, Transplantation of eGFP-labelled SCs from young adult and aged mice that were targeted with shRNAs against *Hoxa9* or a scrambled control. **c**, Representative immunofluorescence staining for Pax7 and eGFP of transplanted muscle sections. Nuclei were counterstained with DAPI (blue). Arrowheads denote Pax7$^+$/eGFP$^+$ cells, asterisks label Pax7$^+$/eGFP$^-$ cells. **d**, Quantification of donor-derived (eGFP$^+$) Pax7$^+$ cells in **c**. **e**, Representative immunofluorescence staining for eGFP and laminin of transplanted muscle sections, nuclei were counterstained with DAPI (blue). **f**, **g**, Quantification of donor-derived (eGFP$^+$) myofibres in **e** for two different *Hoxa9* shRNAs in two independent experiments. **h**, Exemplary immunofluorescence staining for eGFP and laminin in tibialis anterior muscles engrafted with untransduced aged SCs. Nuclei were counterstained with DAPI (blue). **i**, Flow cytometric analysis of transduction efficiency of donor SCs used for transplantation in primary recipients analysed in Fig. 2f. **j**, Representative flow cytometry plots for re-isolation of transplanted aged SCs that were untransduced as control or transduced with scrambled control or *Hoxa9* shRNA encoding lentivirus as quantified in Fig. 2f. **k**, Representative immunofluorescence staining for eGFP and laminin in engrafted tibialis anterior muscles from secondary recipients quantified in Fig. 2g. Nuclei were counterstained with DAPI (blue). Scale bars, 20 μm (**c**), 50 μm (**h**) and 100 μm (**e**, **k**). *P* values were calculated by two-sided Student's *t*-test (**a**, **b**) or two-way ANOVA (**d**, **f**, **g**). $n = 4$ recipient mice in **a**; $n = 3$ mice in **b**; $n = 6$ recipient mice (young donors), $n = 4$ recipient mice (aged donors) in **d**, **f**; $n = 5$ recipient mice in **g**.

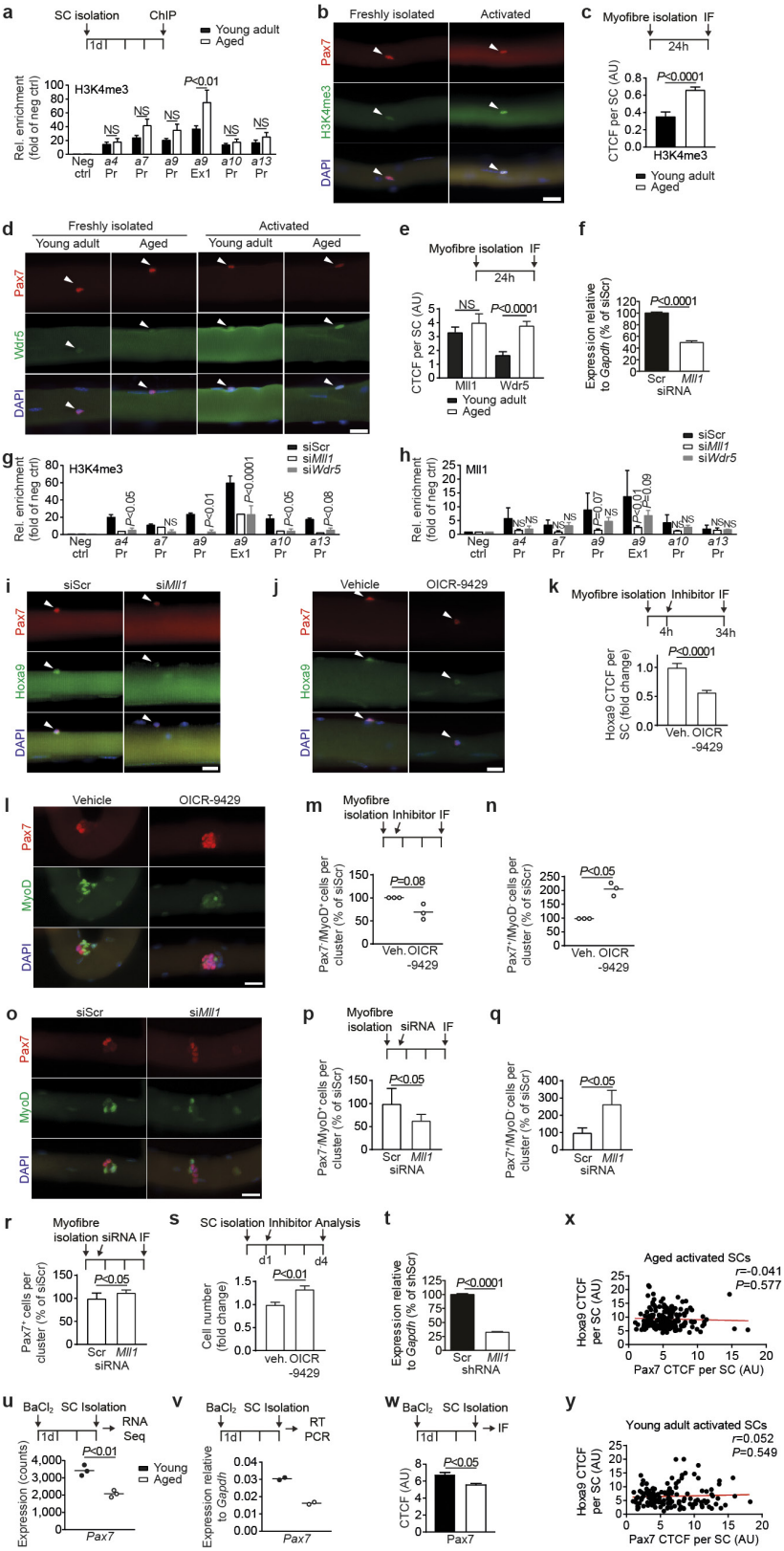

Extended Data Figure 7 | See next page for caption.

Extended Data Figure 7 | Inhibition of Mll1 rescues H3K4me3 induction, *Hoxa9* overexpression, and functional impairment of activated SCs from aged mice. **a**, ChIP for H3K4me3 at promoters or exons of indicated Hox genes in activated SCs (4 day culture) from young adult and aged mice. **b**, Representative immunofluorescence staining for Pax7 and H3K4me3 on myofibre-associated SCs from aged mice that were freshly isolated or activated by 24-h culture of myofibres. **c**, Corrected total cell fluorescence (CTCF) for H3K4me3 on activated SCs shown in **b**. **d**, Representative immunofluorescence staining for Pax7 and Wdr5 on myofibre-associated SCs from young adult and aged mice that were freshly isolated or activated by 24-h culture of myofibres. **e**, CTCF for Mll1 and Wdr5 per activated SC as shown in **d**. **f**, qPCR analysis of *Mll1* in SCs transfected with *Mll1* siRNA or scrambled control. **g**, **h**, ChIPs for H3K4me3 (**g**) and Mll1 (**h**) in primary myoblasts 3 days after transfection with the indicated siRNAs. **i**, **j**, Immunofluorescence staining for Pax7 and Hoxa9 in myofibres from aged mice after transfection with *Mll1* siRNA or scrambled control (**i**, quantification in Fig. 3d) or after treatment with OICR-9429 or vehicle (**j**). **k**, CTCF for Hoxa9 per SC as shown in **j**. **l**, Representative immunofluorescence staining for Pax7 and MyoD on OICR-9429 treated myofibre-associated SCs from aged mice after 72 h culture. Nuclei were counterstained with DAPI (blue). **m**, **n**, Average number of $Pax7^{-}/MyoD^{+}$ cells (**m**) or $Pax7^{+}/MyoD^{-}$ cells (**n**) within clusters as shown in **l**. **o**, Representative immunofluorescence staining for Pax7 and MyoD on siRNA-treated myofibre-associated SCs from aged mice after 72-h culture. Nuclei were counterstained with DAPI (blue). **p**–**r**, Average number of $Pax7^{-}/MyoD^{+}$ cells (**p**), $Pax7^{+}/MyoD^{-}$ cells (**q**) or $Pax7^{+}$ cells (**r**) within clusters in **o**. **s**, Relative changes in cell number of aged SCs after treatment with OICR-9429 and 4 days of culture, compared to vehicle control. **t**, qPCR analysis of *Mll1* in SCs transduced with *Mll1* shRNA or scrambled control. **u**–**w**, Analysis of Pax7 expression in *in vivo* activated SCs from young adult and aged mice by RNA-sequencing (**u**), qPCR (**v**), or immunofluorescence as depicted in Fig. 1b (**w**). **x**, **y**, Pearson correlation comparing the Hoxa9 immunofluorescence signal (quantification in Fig. 1c) and the Pax7 immunofluorescence signal (quantification in **w**) of activated SCs from aged (**x**) and young adult (**y**) mice. Note, there is no correlation between Hoxa9 expression level and Pax7 expression level in activated SCs from aged mice. Scale bars, 20 μm (**b**, **d**, **i**, **j**, **l**, **o**). *P* values were calculated by two-way ANOVA (**a**, **g**, **h**), two-sided Student's *t*-test (**f**, **m**, **n**, **p**–**v**), two-sided Mann–Whitney *U*-test (**c**, **e**, **k**, **w**) or Pearson correlation (**x**, **y**). $n = 4$ mice (young), $n = 7$ mice (aged) in **a**; $n = 27$ nuclei from 2 mice (young), $n = 27$ nuclei from 4 mice (aged) in **c**; $n = 40/52$ nuclei (Mll1), $n = 44/99$ nuclei (Wdr5) from 3 young/aged mice in **e**; $n = 3$ mice in **f**; $n = 3$ biological replicates (*Wdr5* siRNA), $n = 2$ biological replicates (*Mll1* siRNA) in **g**; $n = 3$ biological replicates in **h**; $n = 173$ nuclei (DMSO), $n = 324$ nuclei (OICR-9429) from 4 mice in **k**; $n = 3$ mice in **m**, **n**; $n = 7$ mice in **p**–**r**; $n = 6$ mice in **s**; $n = 3$ mice in **t**; $n = 3$ mice in **u**; $n = 2$ mice in **v**; $n = 134$ nuclei (young), $n = 181$ nuclei (aged) from 3 mice in **w**–**y**.

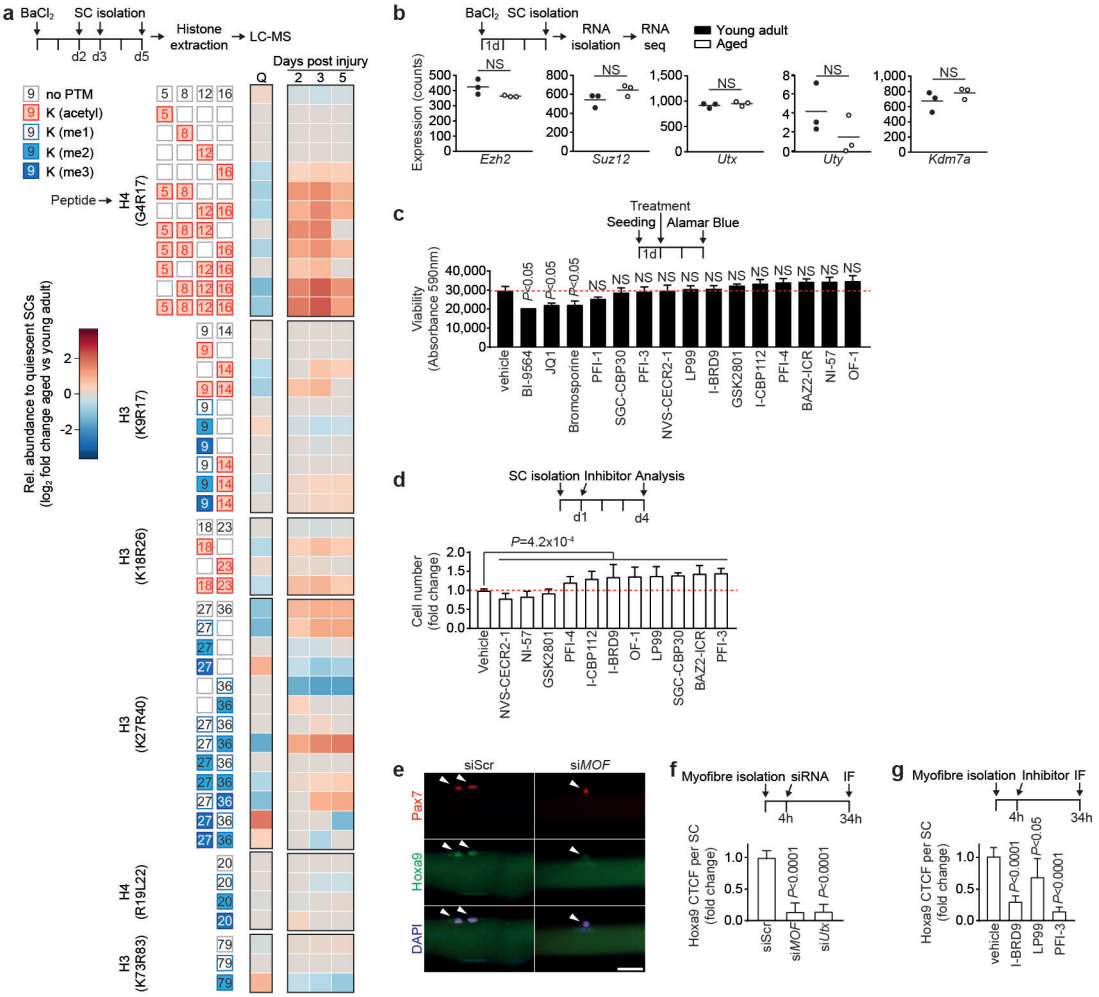

Extended Data Figure 8 | Alterations in the epigenetic stress response of activated SCs from aged mice. a, Heatmap displaying relative changes in abundance of different histone modifications (measured at the indicated peptides) in freshly isolated SCs from aged compared to young adult mice. SCs were analysed in quiescence (Q, derived from uninjured muscle) or at the indicated time points after activation mediated by muscle injury. Relative abundances at indicated days after injury are first normalized to quiescent SCs, and then compared between SCs isolated from aged and young adult mice and $\log_2$ scaled. Only significant changes are shown ($P < 0.05$). **b**, Expression analysis of the indicated genes in freshly isolated *in vivo* activated SCs from young adult and aged mice based on RNA-sequencing. **c**, Viability of primary myoblasts after 48-h treatment with bromodomain inhibitors (1 μM) from the Structural Genomics Consortium probe set, measured by Alamar Blue assay. **d**, Relative changes in cell number of aged SCs after treatment with non-toxic bromodomain inhibitors (1 μM) from **c** and 4 days of culture, compared to vehicle control. A Wilcoxon rank-sum test on the ratio of all cell counts being equal to 1 was performed to test the hypothesis of a general effect of the inhibitors on cell number. **e**, Representative immunofluorescence staining for Pax7 and Hoxa9 in siRNA-treated myofibre-associated SCs from aged mice. Scale bar, 20 μm. **f**, CTCF for Hoxa9 per SC as shown in **e**. **g**, Quantification of immunofluorescence staining for Hoxa9 in $Pax7^+$ cells on myofibre-associated SCs from aged mice treated with bromodomain inhibitors. *P* values were calculated by two-sided Student's *t*-test (**a**–**c**), Wilcoxon rank-sum test (**d**) or two-sided Mann–Whitney *U*-test (**f**, **g**). $n = 4$ mice in **a**; $n = 3$ mice in **b**; $n = 4$ biological replicates in **c**; $n = 6$ mice in **d**; $n = 71$ nuclei (scrambled siRNA), $n = 48$ nuclei (*MOF* siRNA), $n = 98$ nuclei (*Utx* siRNA) from 3 mice in **f**; $n = 60$ nuclei (vehicle), $n = 59$ nuclei (I-BRD9), $n = 38$ nuclei (LP99), $n = 62$ nuclei (PFI-3) from 3 mice in **g**.

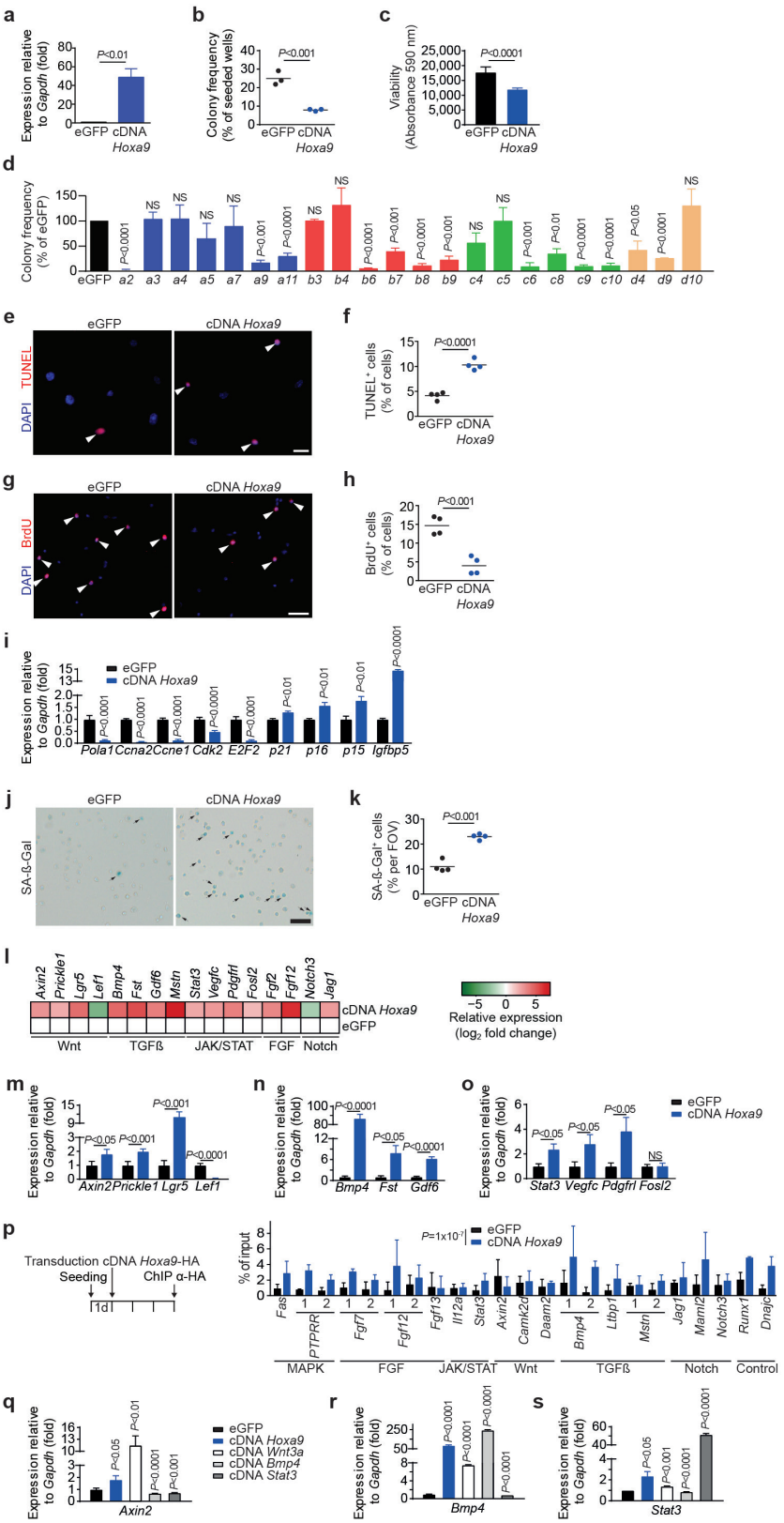

Extended Data Figure 9 | See next page for caption.

Extended Data Figure 9 | Overexpression of *Hox* genes inhibits SC function. a, Expression of *Hoxa9* in SCs transduced with *Hoxa9* cDNA or eGFP as control. **b**, **c**, FACS-isolated SCs from young adult mice were transduced with a lentivirus either containing both eGFP and *Hoxa9* cDNA or only eGFP. Infected ($eGFP^+$) cells were isolated after 3 days. **b**, Frequency of myogenic colonies from single-cell-sorted SCs. **c**, Quantification of cell number based on Alamar Blue assay of bulk cultures. **d**, Frequency of myogenic colonies of SCs overexpressing the indicated Hox genes. **e**, **g**, TUNEL (**e**) or BrdU (**g**) staining of SCs overexpressing *Hoxa9* or eGFP. Infected ($eGFP^+$) cells were isolated 3 days after transduction and analysed 3 days later. Nuclei were counterstained with DAPI (blue). Arrowheads mark TUNEL- or BrdU-positive cells. **f**, **h**, Quantification of apoptosis (**f**) or proliferation (**h**) based on TUNEL or BrdU staining as in **e** or **g**. **i**, qPCR-based expression analysis of various cell-cycle and senescence markers in SCs overexpressing *Hoxa9* compared to eGFP-infected controls, 5 days after infection. **j**, Senescence-associated-β-galactosidase (SA-β-Gal) staining of SCs overexpressing *Hoxa9* or eGFP at day 5 after infection. Arrowheads mark SA-β-Gal-positive cells. **k**, Quantification of senescence per field of view (FOV) based on SA-β-Gal staining in **j**. **l**, Heatmap displaying $\log_2$ fold changes of expression of selected genes from microarray analysis in Fig. 5a. **m**–**o**, qPCR validation of differentially expressed genes annotated to Wnt (**m**), TGFβ (**n**) and JAK/STAT pathways (**o**) as in **l**. **p**, Identification of Hoxa9-binding sites by anti-HA ChIP of primary myoblasts overexpressing HA-tagged *Hoxa9* cDNA or eGFP as control. Shown is the qPCR for 1 or 2 putative Hoxa9-binding sites at the indicated loci. Hoxa9-binding sites at target genes were identified as described in the Methods and are listed in Supplementary Table 1. A two-sided block bootstrap test on the difference of the percentage of bound DNA for all binding sites being equal to 0 was performed to test the hypothesis of a generally increased binding of Hoxa9. **q**–**s**, SCs were infected with lentiviruses expressing *Hoxa9*, *Wnt3a*, *Bmp4* or *Stat3* cDNAs or eGFP. qPCR analysis of expression of the indicated target genes at 5 days after infection: *Axin2* (**q**), *Bmp4* (**r**) and *Stat3* (**s**). Scale bars, 20 μm (**e**, **g**) and 50 μm (**j**). *P* values were calculated by two-sided Student's *t*-test (**a**–**d**, **f**, **h**, **k**, **q**–**s**) or two-way ANOVA (**i**, **m**–**o**). $n = 4$ mice in **a**; $n = 3$ mice in **b**; $n = 7$ mice in **c**; $n = 3$ mice in **d**; $n = 4$ mice in **f**, **h**, **k**; $n = 3$ mice (p15, p21), $n = 6$ mice (p16), $n = 4$ mice (all others) in **i**; $n = 4$ pools of 3 mice in **l**; $n = 4$ mice in **m**–**o**; $n = 3$ biological replicates for **p**; $n = 3$ mice (*Wnt3a*, *Bmp4*, *Stat3*), $n = 4$ mice (eGFP, *Hoxa9*) in **q**–**s**.

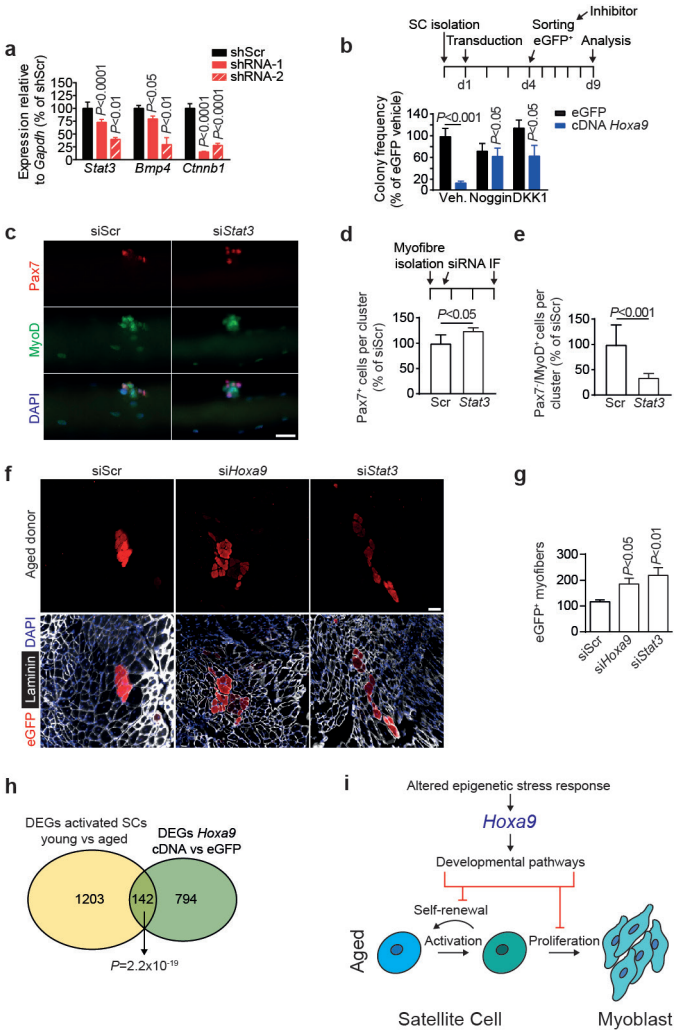

Extended Data Figure 10 | Validation of Hoxa9 downstream targets. **a**, Knockdown efficiency of two shRNAs (red bars) for *Stat3*, *Bmp4* and *Ctnnb1*. **b**, SCs from young adult mice were transduced with an *Hoxa9* and *eGFP*-encoding lentivirus. eGFP$^+$ cells were sorted as single cells and cultured in the presence of noggin, DKK1 or 0.1% BSA in PBS as vehicle. Colony frequency was assessed after 5 days and is compared to *Hoxa9* cDNA expressing cells treated with vehicle control. **c**, Representative immunofluorescence staining for Pax7 and MyoD on siRNA-transfected myofibres from aged mice after 72 h of culture. Nuclei were counterstained with DAPI (blue). **d**, **e**, Average number of Pax7$^+$ cells (**d**) or Pax7$^-$/MyoD$^+$ cells (**e**) within clusters in **c**. **f**, Representative immunofluorescence staining for eGFP and laminin in tibialis anterior muscles engrafted with siRNA-transfected SCs isolated from eGFP transgenic aged mice. Nuclei were counterstained with DAPI (blue). **g**, Quantification of donor-derived (eGFP$^+$) myofibres in **f**. **h**, Area-proportional Venn diagram of differentially expressed genes from indicated transcriptomes. **i**, Model for the Hoxa9-mediated impairment of SC function during ageing: quiescent SCs become activated upon muscle injury and proliferate as myoblasts to repair damaged muscle tissue. After activation, aged SCs display global and locus-specific alterations in the epigenetic stress response resulting in overexpression of *Hoxa9*, which in turn induces developmental pathways inhibiting SC function and muscle regeneration in aged mice. Scale bars, 20 μm (**c**), and 100 μm (**f**). *P* values were calculated by two-way ANOVA (**a**, **b**) or two-sided Student's *t*-test (**d**, **e**, **g**). $n = 3$ mice in **a**; $n = 4$ mice in **b**; $n = 5$ mice in **d**, **e**; $n = 5$ recipient mice in **g**; $n = 3$ mice per group (activated SCs), $n = 4$ pools of 3 mice (*Hoxa9* overexpression) in **h**.